Fracture Mechanics of Concrete and Concrete Structures - Recent Advances in Fracture Mechanics of Concrete - B. H. Oh, et al.(eds)

A mesoscopic approach for a better understanding of the transition from diffuse damage to localized damage

C. La Borderie, C. Lawrence, T.D. N'Guyen,
LaSAGeC2, University of Pau, Anglet, France

T. D. N'Guyen, G. Nahas,
IRSN/DSR/SAMS/BAGCS, France

ABSTRACT: The aim of this paper is to present a modeling of mechanical behavior of concrete at a mesoscopic scale, in 2 and 3 dimensions. Concrete is considered as a bi-phasic material where the cement paste and the aggregates are described with their own mechanical characteristics. The aggregates are idealized with circular shapes (discs in 2D, spheres in 3D). The aggregates are randomly placed into the concrete specimen, conforming to the aggregates size distribution curve and the aggregate / paste area ratio. In a first time, the model is studied in two dimensions in order to optimize the geometrical model of the inner structure of concrete in terms of the meshing strategy and the smallest size of the aggregate to take into account. An original method to mesh the mesoscopic geometry of concrete has been developed with diffuse mesh, and the results of the 2D model are analyzed and compared in tension and compression. A first interesting result is that the model can exhibit dilatancy of concrete in compression even when a simple damage model (without plasticity nor inelastic strains) is used. The model shows as well interesting results on the transition from diffuse to localized damage. Finally, results of the tridimensional model are shown in tension.

1 INTRODUCTION

A major issue for concrete structures is cracking control, so that a major issue for concrete modeling is to predict the transition from diffuse damage to localized damage. Therefore, cracking in concrete begins with diffuse micro-cracks (lots of micro-cracks with small openings) and then localizes into macro-cracks (few fractures with larger openings). Concrete behavior is totally different between these two phases, particularly towards permeability. The transition is driven by the heterogeneities of the material : this is why we have chosen a mesoscopic scale model. This model is used to better understand the concrete behavior and will be integrated into a multi-scale computation process.

2 MECHANICAL BEHAVIOR MODEL FOR CONCRETE COMPONENTS

Macroscopic models generally have a lot of parameters to describe the complex mechanical behavior of concrete. Since we suppose that most of this complexity can be represented by the inner geometry of the material, we chose for paste or aggregate a mechanical behavior model as simple as possible, based on a Mazars model's (Mazars, 1984). The contact between paste and aggregates is considered as perfect (no joint elements and kinematic continuity). The used behavior model is the Fichant's model (Fichant et al., 1999) which can control fracture energy Gf and takes into account the crack closure effects. The plasticity should be activated if necessary and damage effects in compression are decreased.

This simple model represents unilateral effects and is regularized by a Hillerborg's method.

Material parameters are given in table 1.

	E (GPa)	f_t (MPa)	G_f (N.m)	ν
Paste	15	3	20	0.2
Aggregates	60	6	60	0.2

Table 1 : Mechanical characteristics of paste and aggregates

3 MESOSTRUCTURE GENERATION

The evaluation of the composite behavior of concrete at mesoscopic level requires the generation of a numerical concrete with an aggregate structure, which consists in randomly distributed aggregates

and cement matrix filling the space between the particles. The matrix or paste eventually contains the smallest aggregates, depending on the fineness of the description of aggregates, and its layout depends entirely on the spatial distribution of aggregate particles.

A diffuse meshing method with projection of the heterogeneous material properties on the shape functions of a finite element mesh (regular or not) has been used in this study because it is easy to deal with, it does not introduce irregularities in the interface between the cement paste and aggregates that are not representative of the real geometry.

The numerical concrete model is developed in two or three dimensions with discs or spheres randomly distributed according to a given particle size distribution curve. We use a classic logarithmic distribution of class size and choose 12 or 11 classes to describe the aggregates.

The size of the aggregates and their distribution into the material involves different correlation lengths that affect the damage distribution during the cracking process. We choose to study a concrete whose diameter of the coarsest aggregates is 25 mm, the size of the specimen is of 100 mm and the element size is 0.4 mm (in 2D) or 1.25 mm (in 3D) (that is to say 63,001 nodes in 2D or 330,675 nodes in 3D). In order to have a correct description of the geometry, the smallest size of aggregate taken into account is of 1.25mm and the matrix represents the cement paste and aggregates smaller than this limit. Knowing the volume percentage of the particle size distribution of aggregates (assuming same density of all aggregates, issued from same rocks) and the total volume of aggregates in concrete sample, the number of circular aggregates of each granular class can be easily calculated using the unit volume of aggregates of each size i. To avoid boundary effect which automatically increases the volume of matrix between aggregates, the inclusions are placed in a larger sample, from the largest to the smallest aggregates, without overlap, and with final cut of all particles parties outside the concrete specimen. Examples of meshes in are given in figure 1.

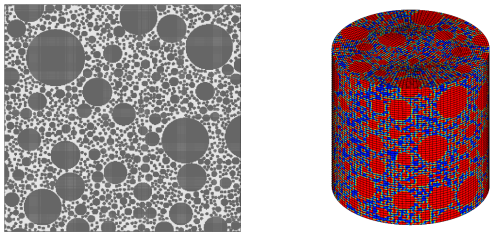

(a) (b)

Figure 1 : Example of mesoscopic geometries (a) 2D (b) 3D

4 LOADING AND BOUNDARY CONDITIONS

Numerical samples are tested in uni-axial compressive and uni-axial tensile tests with the Finite Element code CAST3M. In 2D, due to the small sample size, we set pseudo periodic conditions (symmetry on the edges AB and DA) that allow us to keep the edge BC free. We impose a displacement jump Δ at the edge CD. In 3D, we impose a displacement jump Δ at the face S2. The loading and boundary conditions are illustrated on figure 2.

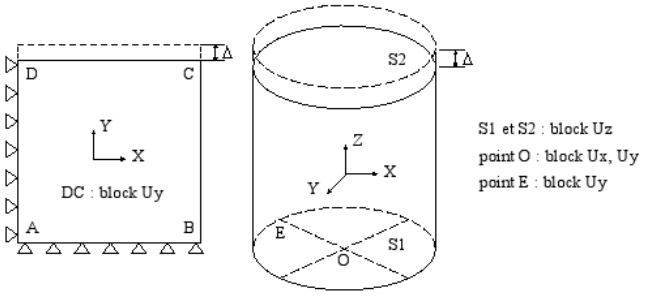

in 2D in 3D

Figure 2. Loading and boundary conditions

5 SIMULATIONS RESULTS IN 2D

5.1 *Global results*

The macroscopic values Σ_{ij} and E_{ij} of the stress and the strain are defined by their respective volumetric means on the specimen. Computed stress strain curves $\Sigma_{ij} - E_{ij}$ (fig. 3) accurately describe deterioration of concrete in tension and in compression. In tension, Gf calculated from the constitutive relation $\Sigma yy - Eyy$ is 71.7 J/m^2 which is much greater than the value given for the cement paste (20 J/m^2) because of the energy dissipation which occurs in micro-cracking into the fracture process zone. In compression, although the model does not contain any information about volumetric strains but only an almost elastic linear law in pure compression at macroscopic level, it manages to describe successive stages in compression for volumetric strains: contraction then expansion, due to the precise geometric description of the mesostructure.

The influence of the draw in the random distribution of aggregate on the behavior of the numerical concrete is low. : for different draw, curves are superimposed before the peak, and then gaps between the curves remain small after the peak. Moreover the Gf magnitude is fine.

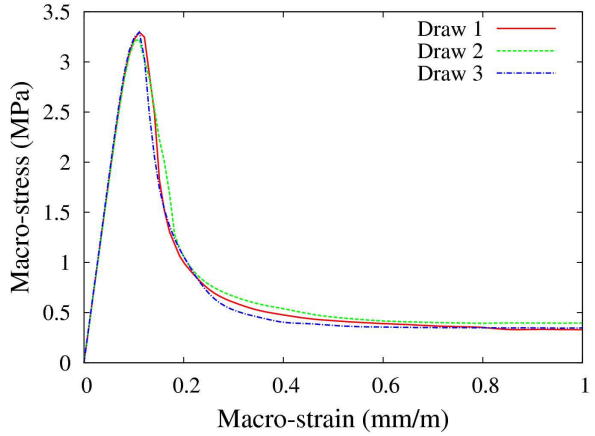

in tension

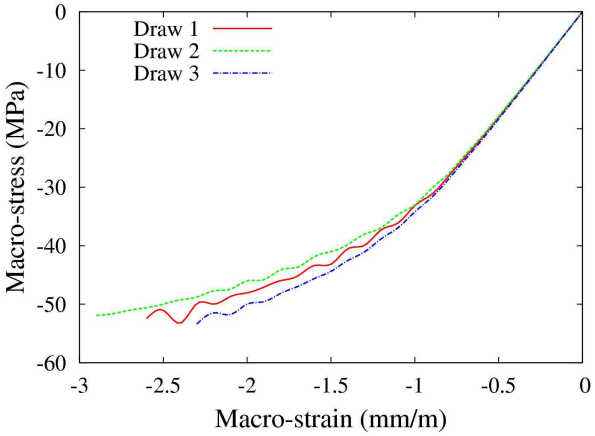

in compression

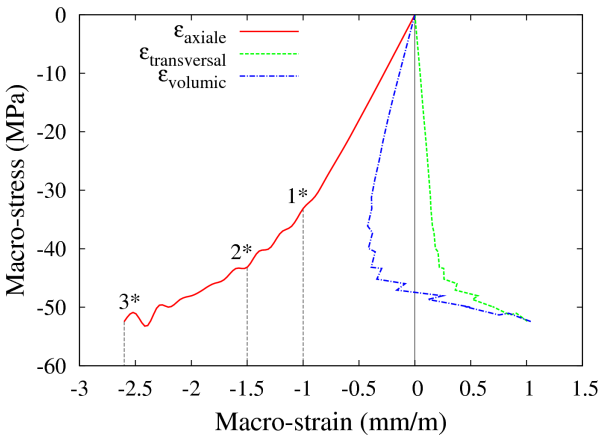

in compression with volumetric strain

Figure 3. Curves behavior of concrete for three different meshes for 0-25mm concrete with 12 classes aggregates (smallest class : 0-2.5 mm), paste / aggregate ratio 71%

5.2 *Local results*

At a local level, crack openings are studied with two hypotheses: a damaged element is crossed over by a single crack and uncracked material is elastic (Boussa et al., 2001). Strain ε for size h element load by a stress σ is composed of an elastic strain ε_o in the element and a displacement jump δ represented by unitary crack opening tensor ε_{ouf} (Matallah et al., 2009; Ragueneau et al., 2000).

Damage allows to represent zones where energy has been dissipated (fig. 5) whereas active damaged zones should be represented by δ_{kk} , the first invariant of the crack opening tensor δ_{ij} (La Borderie et al., 2007) (fig. 4). The crack openings depends on damage and on the local state of stress. When the stress vanishes or is reversed, some cracks may close. The position of the cracks crossing the elements can be found and can be used with their respecting openings for others computations on permeability of damaged concrete as an example (fig. 5-6) .

For the tension test, one single macrocrack develops whatever the mesh , the crack pattern is perpendicular to the axis of loading Oy . Damage is first distributed, then it continues to be diffused after the peak, and it localizes finally in a single macro-crack. Moreover, we observe that the cracks appear at the interface of cement paste / aggregate, and then propagate within the cement paste. Most of the microcracks created at the beginning of the test are quite closed at its end. These observations are conform with experiments (fig. 4).

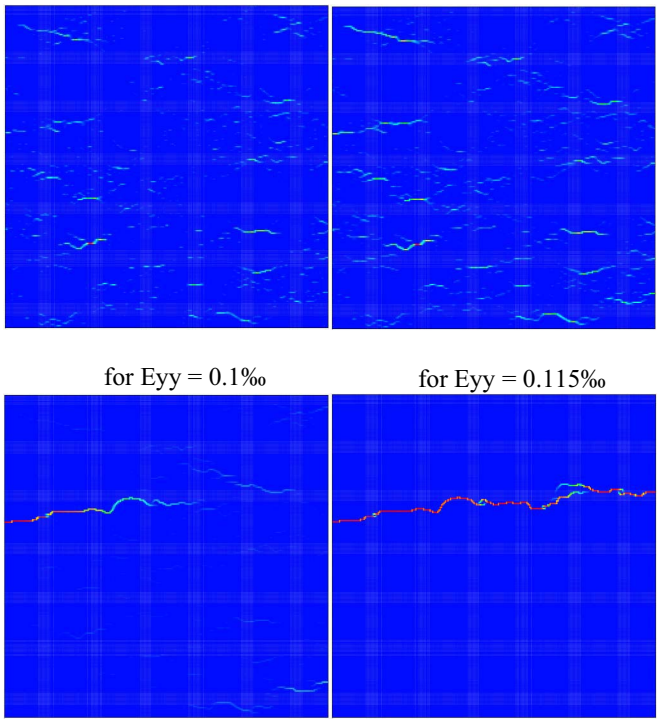

Figure 4. δkk : Active damaged zone in tension for 2D mesh given in figure 1

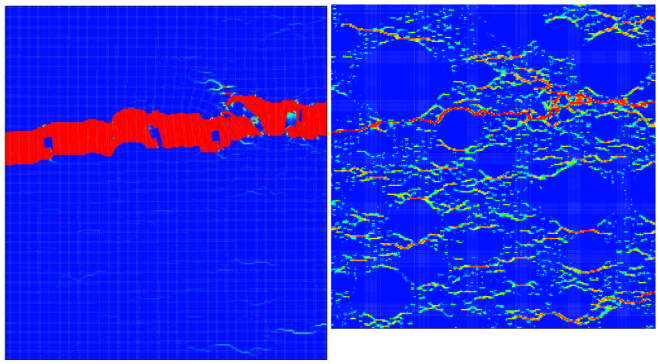

Crack opening of concrete Damage field

Figure 5. Local results for Eyy = 1‰ in tension for 2D mesh given in figure 1

For the compression test (fig. 6), the cracks develop in a similar way whatever the draw : the direction of the cracks is at about ±20◦ from the loading axis. Cracks are complex and some aggregates go to failure. It leads to the breakdown of the concrete specimen at the free [BC] edge. These observations are conform with experiments.

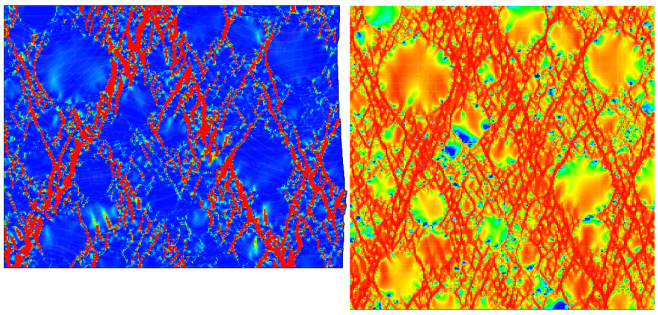

Crack opening of concrete Damage field

Figure 6. Local results for Eyy = 2.5‰ in compression for 2D mesh given in figure 1

5.3 *Conclusions*

The mesoscopic model has been developped in two dimensions with a geometric accuracy of about 1 mm and an element size of 0.4 mm. The computated behavior in tension and compression is similar to that observed in experiments as well at the global level than at the local level. The transition from diffuse damage to localized damage is described and can be compared with experiments. The repeatability of the model is good as shown of figure 3 for global results.

In the next paragraph, we will examine some ways to use this approach with a coarser mesh in order to perform tridimensional computations.

6 INFLUENCE OF FINENESS OF THE DISCRETIZATION ON THE BEHAVIOR OF THE NUMERICAL CONCRETE IN 2D

6.1 *Influence of fineness*

If we want to use a coarser mesh, the smallest aggregates couldn't be correctly represented. We evaluate here the role of the smallest agregates on the behavior of concrete.

Two additional numerical concrete are used. The first one (named B11-55) uses only the 11 larger classes of aggregates, the aggregate paste ratio decreases at 55% instead of 71%. The second one (B11-71) is also based on the 11 larger classes but ne number of aggregates of it's smaller class is increased so that the aggregate paste ration remains at 71%. Note that in this part, the same parameters are used for the paste parameters.

The influence of fineness of the discretization on crack pattern of the numerical concrete is low, see fig. 5,6 for the B12-71, fig. 7 for the B11-71 and fig. 8 for the B11-55 . Whatever the aggregates representation, final macrocracks are similar but the cracking process differs slightly at the beginning of microcracking.

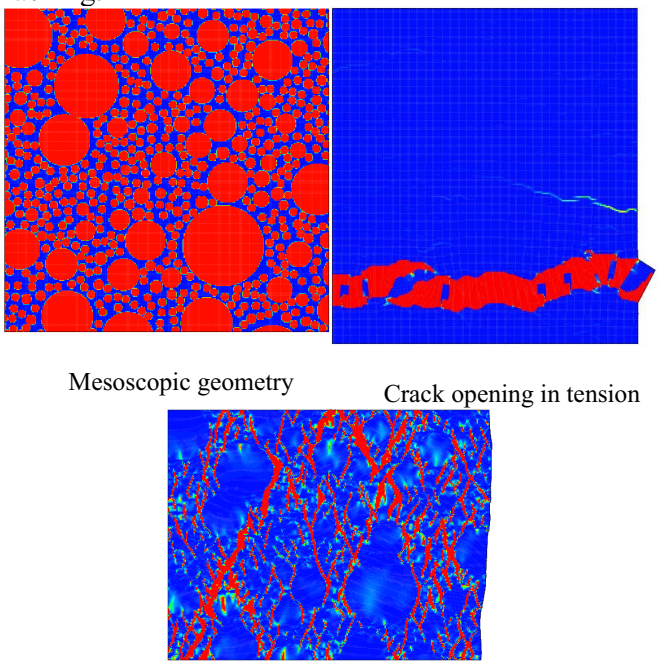

Mesoscopic geometry Crack opening in tension

Crack opening in compression

Figure 7. Behavior of the B11-71 concrete

The different global results given by the macro stress strain relation are presented on fig. 9. The macroscopic behavior in tension is slightly dependent on the presence of small aggregates and on the aggregate-paste ratio, it is predominantly governed by the positions of the coarsest aggregates.

The influence of the aggregate-paste ratio and of the smallest aggregates seems to be higher on compression.

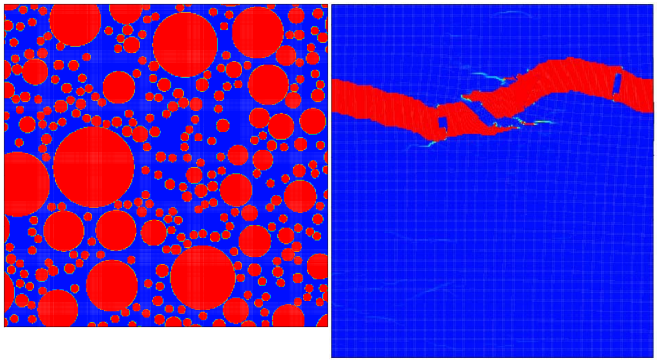

Mesoscopic geometry

Crack opening in tension

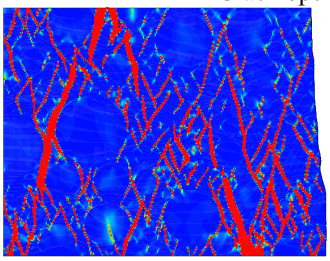

Crack opening in compression

Figure 8. Behavior of the B11-55 concrete

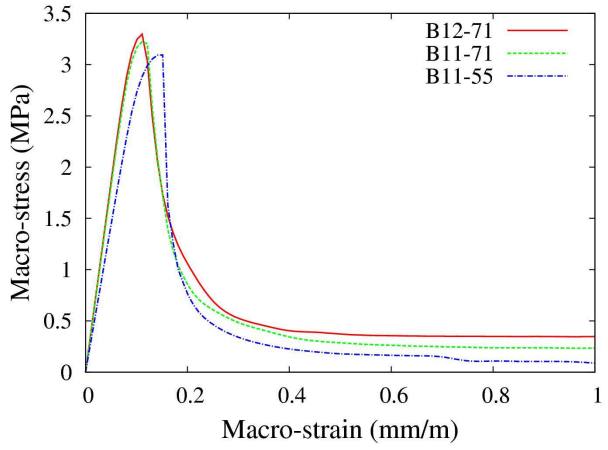

In tension

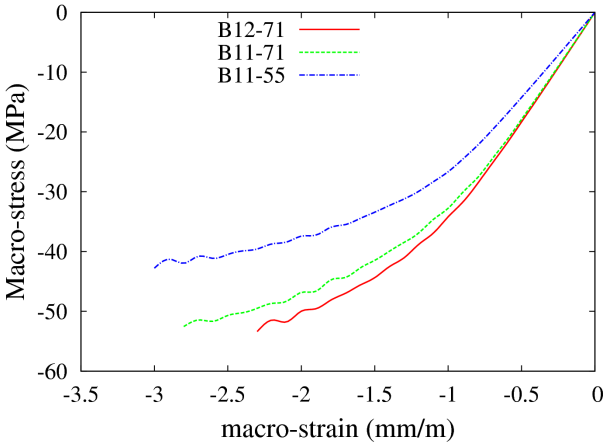

In compression

Figure 9. Curves behavior of B12-71, B11-71 and B11-55 concretes

In order to quantify these results, we propose to compare the energy dissipated into the material in tension : $G_f^t = \int \Sigma \, dE$ and in compression $G_f^c = \int \Sigma \, dE$. These results are reported in table 2, the relative deviation from the B12-71 results are mentioned.

	$G_f^t J/m^2$	$G_f^c J/m^2$	ΔG_f^t	ΔG_f^c
B12-71	71.7	7709	-	-
B11-71	63.3	7289	-1.3	-7.3
B11-55	52.7	5857	-31.6	-25.8

Table 2 : dissipated energy in tension and compression

The role of the aggregate-paste ratio is more important that the one of the smallest aggregates.

The relative deviation obtained for the B11-55 concrete in important, for this concrete, the paste contains the smallest aggregates and their effect was not taken into account.

6.2 *Interaction between smallest aggregates and others*

Th B11-55 concrete has less aggregates than the others, for this concrete, the characteristics of the matrix should be identified from another computation with the paste and only the 0-1.25 mm aggregates, using material parameters given in table 1. As shown on figure 10, this computation gives f_t = 3.6 MPa and G_f = 26.3 J/m2.

A new computation with these parameters for the matrix, is performed for the B'11-55 concrete. One can suppose that the participation of the smallest aggregates in the fracture energy of the concrete are included in the increasing of the matrix characteristics. The value obtained for the B'11-55 G_f is 65.5 J/m^2 instead of 71.7 J/m^2.

As all the non-linearities appear only in the matrix, the obtained fracture energy can be split in the part due to the matrix, and the geometric part due to the heterogeneities. The contribution of the matrix increases from 20J/m^2 to 26.3J/m^2 as the geometric contribution decreases from 51.7J/m^2 to 39.2J/m^2 .The difference probably comes from the interactions between smallest aggregates and others that cannot be taken into account with this multi-scale approach.

These results are summarized in the fig. 10.

	E (GPa)	f_t (MPa)	G_f (J/m2)	ν
Paste 1	15	3	20	0.2
Aggregates	60	6	60	0.2

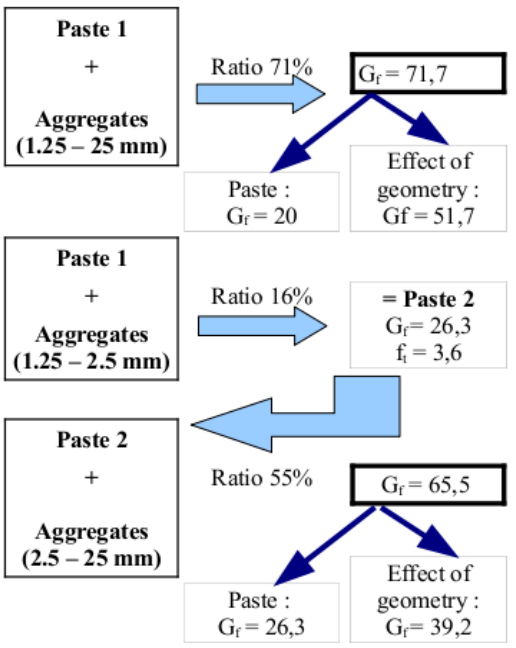

Figure 10 : effects of the geometry on Gf in tension

7 SIMULATIONS RESULTS IN 3D

To perform 3D computations, the specimen is 100 mm in diameter and 100 mm height cylinder (Figure 6d and Figure 7b) and is subjected to tension or compression. The size of the elements is lower than 1.25 mm and the mesh contains 330,675 nodes. The distribution of aggregates was done according to the B11-71.

7.1 *In tension*

The results of the numerical concrete specimen in tension in 3D are presented in figure 11 and figure 12. We note that the curve Σyy − Eyy is quite representative of a concrete in tension. The tensile strength and the fracture energy (157.37J/m2) is higher than that obtained from 2D computations due to a more complex geometry of the crack pattern in 3D (the material modeled with the 2D mesoscopic model is in fact composed of cylindric inclusions). The crack pattern remains perpendicular to the axis of tensile loading Oz. Cracking starts at the aggregate boundaries and is first distributed in the whole specimen, then it continues to be diffused after the peak, and finally, it localizes in a single macro-crack.

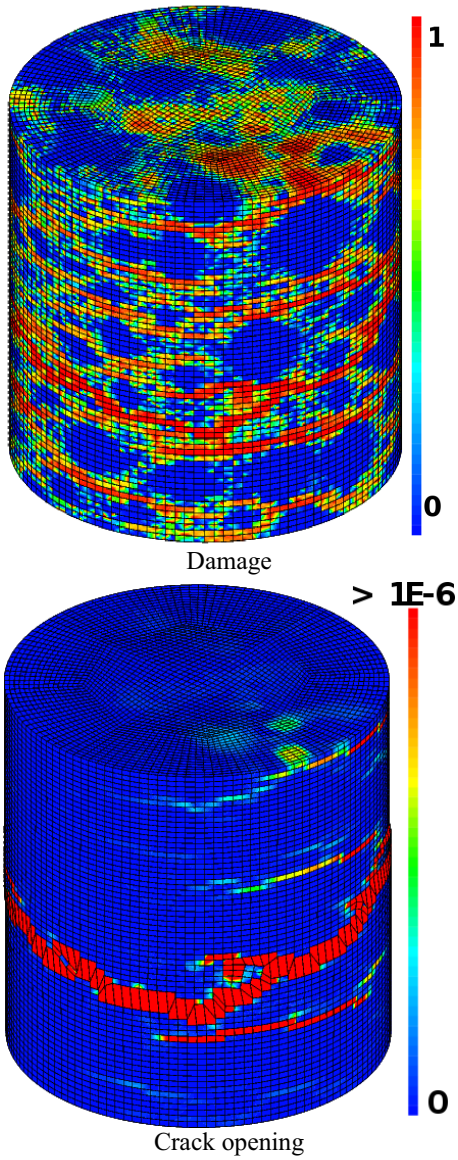

Figure 11.Local results in tension in 3D

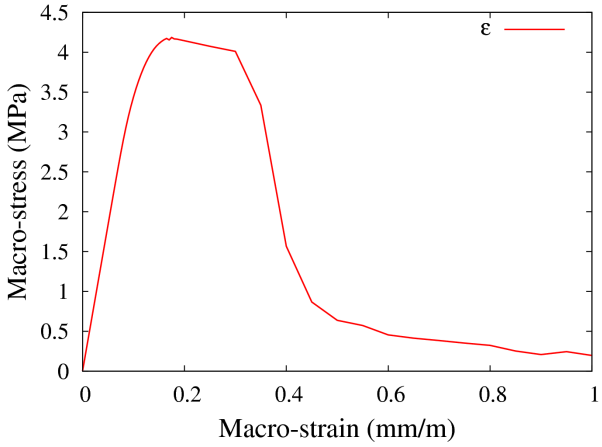

Figure 12. Curve behavior of concrete in tension in 3D

8 CONCLUSIONS

Computations are made on the mesoscopic scale with a quite simple mechanical model coupled with a precise description of heterogeneity on sand grain scale. A numerical concrete is randomly generated from the aggregates grading curve, and a diffuse mesh used to compute uniaxial tension and uniaxial compression loading testing. The macroscopic responses ($\Sigma ij - Eij$ curves), the damage distributions and the crack opening are presented and show the accuracy of this mesoscopic approach to bridge continuous and discrete results in order to model the onset and the propagation of cracking, and in the meantime to provide crack indicators (spacing and opening).

Moreover, two interesting results are obtained :

– Compression damage is correctly described even in terms of volumetric strains.

– The model describes accurately the failure process in concrete. This process is characterized by gradual transition from diffuse damage, strain and micro-cracking to strain localization, and finally to a macroscopic crack.

These mechanisms can not be described with a macroscopic approach.

Besides, it has been shown that the influence of the distribution of aggregates and the influence of fineness of the discretization are low until the aggregate / paste area ratio is constant and that the aggregate / paste area ratio is important for the accuracy of the modeling in term of global results.

Therefore, this mesoscopic model has proven to be a very practicable and useful approach for studying the influence of the concrete composition on the macroscopic properties and also to gain insight into the origin and nature of the nonlinear behavior of concrete.

The model is completely 3D capable and the accuracy of results should be better in 3D, unfortunately the computations are even time consuming and efforts must been made in the optimization of the process in 3D.

Future work will focus on three dimensional computations, and on modeling the flow in the cracked concrete.

REFERENCES

Aydin A. C., Arslan A., Gul R., " Mesoscale simulation of cement based materials, time-dependent behavior", Computational Materials Science, vol. 41, p. 20-26, February, 2007.

Bentz D., " Three-dimensional computer simulation of portland cement hydration and microstructure development", Journal of the American Ceramic Society, vol. 80, n° 1, p. 3-21,1997. cited By (since 1996) 111.

Boussa H., Lawrence C., Borderie C. L., " A Model for computation of Leakage Through Damaged Concrete Structures", Cement and Concrete Composites, vol. 23, p. 279-287, Avril, 2001.

Caballero A., Lopez C., Carol I., " 3D meso-structural analysis of concrete specimens under uniaxial tension", Computer Methods Applied Mechanics and Engineering, vol. 195, n° 52, p. 7182-7195, 2006.

Ciancio D., Carol I., Cuomo M., " Crack opening conditions at 'corner nodes' in FE analysis with cracking along mesh lines", Engineering Fracture Mechanics, vol. 74, p. 1963-1982, 2007.

Comby Perrot I., Development and validation of a 3D computational tool to describe damage and fracture due to alkali silika reaction in concrete structures, Phd thesis, École des mines de Paris, 2006.

De Sa C., Étude Hydro-Mécanique et Thermo-mécanique du Béton - Influence des gradients et des incompatibilités de déformation, Phd thesis, École Normale Supérieure de Cachan, 2007.

Fichant S., La Borderie C., Pijaudier-Cabot G., " Isotropic and Anisotropic Descriptions of Damage in Concrete Structures", Mechanics of Cohesive-Frictional Material, vol. 4, n° 4, p. 339-359, Juillet, 1999.

Gogard V., Modélisation de l'endommagement anisotrope du béton avec prise en compte de l'effet unilatéral : Application à la simulation des enceintes de confinement nucléaires, Phd thesis, Université Pierre et Marie Curie, 2005.

Grondin F. A., Modélisation Multi-Échelles du Comportement Thermo-Hydro-Mécanique des Matériaux Hétérogènes. Applications aux Matériaux Cimentaires sous Sollicitations Sévères, Phd thesis, Université Pierre et Marie Curie, Décembre, 2005.

Hafner S., Eckardt S., Luther T., Konke C., " Mesoscale modeling of concrete: Geometry and numerics", Computers and Structures, vol. 84, p. 450-461, 2006.

Hager I. G., Comportement à haute température des bétons à haute performance - évolution des principales propriétés mécaniques, Phd thesis, l'École Nationale des Ponts et Chaussées et l'École Polytechnique de Cracovie, Novembre, 2004.

La Borderie C., Stratégies et Modéles de Calculs pour les Structures en Béton, Habilitation à diriger les recherches, Université de Pau et des Pays de l'Adour, Décembre, 2003.

La Borderie C., Lawrence C., Menou A., " Approche mésoscopique du comportement: Apport de la représentation géométrique", Revue Européenne de Génie Civil, vol. 11, n° 4, p. 407- 421, 2007.

Ladevèze P., Sur une Théorie de l'Endommagement Anisotrope, Technical Report n° 34, Laboratoire de Mécanique et Technologie, École Normale Supérieure de Cachan, mars, 1983.

Leite J. P. B., Slowik V., Apel J., " Computational model of mesoscopic structure of concrete for simulation of fracture processes", Computers and Structures, vol. 85, p. 1293-1303, 2007.

Matallah M., Borderie C. L., " Inelasticity-damage based model to numerical modeling of concrete cracking", Engineering Fracture Mechanics, vol. 76, n° 8, p. 1087-1108, 2009.

Mazars J., Application de la Mécanique de l'Endommagement au Comportement Non-Linéaire et à la Rupture du Béton de Structures, Doctorat d'état, Université Paris 6, 1984.

Mazars J., " A Description of Micro and Micro Scale Damage of Concrete Structure", Journal of Engineering Fracture of Mechanics, vol. 25, n° 5–6, p. 729-737, 1986.

Mazars J., Pijaudier-Cabot G., " From damage to fracture mechanics and conversely: A combined approach", International Journal of Solids and Structures, vol. 33, n° 20-22, p. 3327 - 3342, 1996.
Menou A., Étude du comportement thermomécanique des bétons à haute température : approche multi échelles de l'endommagement thermique, Phd thesis, Université de Pau et des Pays de l'Adour, Janvier, 2004.
Mounajed G., Expérience, théorie at modèles numériques : Des méthodes combinées pour l'étude du comportement multiphysiques et multi-échelles des structures et matériaux, Habilitation à diriger les recherches, Université Paris VI, Décembre, 2004.
Mounajed G., Menou A., Boussa H., La Borderie C., Carré H., " Multi-scale approach of thermal damage : application to concrete at high temperature", International Conference on Fracture Mechanics of Concrete and Concrete Structures, vol. 1, Vail Colorado, USA, p. 513-520, 2004.
Nagai K., Sato Y., Ueda T., " Mesoscopic Simulation of Failure of Motar and Concrete by 2DRBSM", Journal of Advanced Concrete Technology, vol. 2, n° 3, p. 359-374, 2004.
NIST, " Object Oriented Finite Element Analysis of Real Material Microstructure Working Group", 1998.
Prado E., Van Mier J. G. M., " Effect of particle structure on mode I fracture process in concrete", Engineering Fracture Mechanics, vol. 70, n° 14, p. 1793-1807, 2003.
Ragueneau F., La Borderie C., Mazars J., " Damage model for concrete-like materials coupling cracking and friction, contribution towards structural damping: first uniaxial applications", Mechanics of Cohesive-Frictional Materials, vol. 5, n° 8, p. 607-625, 2000.
Réthoré J., Hild F., Roux S., " Shear-band capturing using a multiscale extended digital image correlation technique", Computer Methods in Applied Mechanics and Engineering, vol. 196, n° 49-52, p. 5016 - 5030, 2007.
Roelfstra P. E., A numerical approach to investigate the properties of concrete. Numerical concrete, Phd thesis, École Polytechnique Fédérale de Lausanne, 1989.
Souid A., Delaplace A., Ragueneau F., Desmorat R., " Pseudo-dynamic testing and nonlinear substructuring of damaging structures under earthquake loading", Engineering Structures, vol. 31, n° 5, p. 1102 - 1110, 2009.
Wang Z. M., Kwan A. K. H., Chan H. C., " Mesoscopic study of concrete I: generation of random aggregate structure and finite element mesh", Computers and Structures, vol. 70, p. 533-544, 1999.
Wang Z. M., Kwan A. K. H., Chan H. C., " Mesoscopic study of concrete II: nonlinear finite element analysis", Computers and Structures, vol. 70, p. 545-556, 1999.
Wittmann F. H., Roelfstra P. E., L. K. C., " Drying of concrete : An application of the 3L-approach", Nuclear Engineering and Design, vol. 105, n° 2, p. 185-198, 1988.
Wriggers P., Moftah S. O., " Mesoscale models for concrete: Homogenisation and damage behaviour", Finite Elements in Analysis and Design, vol. 42, p. 623-636, 2006.